Journal of Electroanalytical Chemistry 757 (2015) 23–28

Contents lists available at ScienceDirect

Journal of Electroanalytical Chemistry

journal homepage: www.elsevier.com/locate/jeac

Selective and sensitive electrochemical determination of Pb^{2+} based on highly adsorptive WOx–ethylenediamine nanowires

Miaoqi Li, Jie Wu, Lin Cui, Huangxian Ju *

State Key Laboratory of Analytical Chemistry for Life Science, School of Chemistry and Chemical Engineering, Nanjing University, Nanjing 210093, PR China

ARTICLE INFO

Article history:
Received 20 July 2015
Received in revised form 28 August 2015
Accepted 1 September 2015
Available online 5 September 2015

Keywords:
Electrochemical sensor
Chemically modified electrode
WOx–ethylenediamine hybrid nanowires
Heavy metal ion
Lead ion

ABSTRACT

Inorganic–organic hybrid WO*x*–ethylenediamine (WO*x*–EDA) nanowires with high surface-to-volume ratio and abundant amino groups were synthesized for selective and sensitive electrochemical determination of Pb^{2+}. The WO*x*–EDA nanowires possessed a uniform lamellar mesostructure and could disperse evenly in Nafion solution for preparation of WO*x*–EDA modified electrode with good reproducibility. The modified electrode showed selective response toward Pb^{2+} due to the chelating between amino groups and Pb^{2+}. The electrochemical characterization and detection of bound Pb^{2+} were performed by square wave anodic stripping voltammetry. Under optimized conditions, the WO*x*–EDA-based sensor could detect Pb^{2+} directly from 0.01 to 10 μM with a detection of limit down to 3.2 nM. The proposed sensor with WO*x*–EDA hybrid nanowires exhibited good selectivity and sensitivity, and acceptable stability and reproducibility, showing promising practical application in Pb^{2+} determination.

1. Introduction

Heavy metal ions are well-known undesirable constituents in drinking water, since they are barely biodegradable and can be accumulated in the human body through the food chain to induce a severe threat to human health [1,2]. As one of the most common heavy metal ions, lead can damage the functionality of the central nervous system, hematopoietic system and kidney even at low concentration, and cause various severe or fatal consequences (especially in children) [3]. Because of the significant hazard, it is of great importance to develop selective and sensitive detection strategies for toxic heavy metal ions with cost-effective and convenient procedures. So far, several elegant techniques have been developed, including atomic absorption/emission spectrometry [4], inductively coupled plasma mass spectrometry [5], colorimetric spectrometry [6], fluorescence spectrometry [7] and electrochemical method [8]. Among them, the electrochemical detection method has been widely developed due to its capability of short analytical time, low power consumption, high sensitivity, inherent simplicity and ease of miniaturization for *in-situ* measurement [9,10]. Particularly, anodic stripping voltammetry (ASV) has been proved to be an extremely powerful technique for detecting trace level of elements in distinct oxidation states [11–16]. However, it still remains a great challenge to improve the selectivity of the electrochemical sensors for specific metal ions. Therefore, the strategy of inducing metal ion-specific functional groups onto the electrode surface has emerged to meet the demand.

Organic functional groups, including thiol [17], amino [18,19], carboxylic [20,21], hydroxyl [22] and sulfur groups [23], generally possess strong complexation or chelating ability toward heavy metal ions, and have been frequently applied to nanomaterial functionalization to enhance their selectivity in stripping voltammetry. For example, multiwalled carbon nanotubes functionalized with cryptand [2.2.1], thiolated chitosan, and carbon dots (C-Dots) functionalized with N-(2-aminoethyl)-N,N′,N′-tris-(pyridine-2-yl-methyl)ethane-1,2-diamine (AE-TPEA) were utilized for the selective detection of Cu^{2+}, Hg^{2+} and Bi^{2+}, respectively [24–26]. However, surface functionalization mostly involves post-synthetic grafting steps, which generally requires expensive organic precursors for grafting, tedious and complicated procedures and harsh experimental conditions [27,28]. Therefore, it was highly desirable to develop electrochemical sensors based on new materials with inherent selective adsorption toward specific metal ions.

Recently, some inorganic metal oxides or hydroxides with highly selective adsorption toward specific metal ions were successfully used for enhancing selectivity in stripping voltammetric detection [9,29]. For example, Fe_3O_4 microspheres offered direct detection of arsenic (III) with high selectivity and sensitivity. Nanostructure Mg–Al-layered double hydroxides were found to be useful for the selective detection of cadium (II). Recently, inorganic–organic hybrid materials which integrate the superior rigidity and thermal stability of the inorganic framework with the structural diversity, flexibility and functionality of organic components have attracted great attention due to their excellent adsorption, easy fabrication, environmental friendliness, and rich surface groups. Inorganic–organic hybrid WO*x*–ethylenediamine (WO*x*–EDA) nanowires produced by intercalation of ethylenediamine into WO_6 octahedra layers possess abundant amino groups and have been reported

---

* Corresponding author.
E-mail address: hxju@nju.edu.cn (H. Ju).

http://dx.doi.org/10.1016/j.jelechem.2015.09.001
1572-6657/

to show exceptionally higher adsorption capacity toward Pb^{2+} than other metal ions with a maximum adsorption capacity of 925 mg g^{-1} [28].

Herein, the WOx–EDA hybrid nanowires were employed to prepare an electrochemical sensor for highly selective and sensitive determination of Pb^{2+}. The WOx–EDA nanowires could be easily synthesized and well dispersed in Nafion film for modification of electrode surface. Due to the high surface-to-volume ratio and strong chelating effect between amino groups and Pb^{2+}, the WOx–EDA-based sensor could selectively detect Pb^{2+} in the presence of most other metal ions at ten times higher concentration, along with a detection limit down to nM level. Benefiting from the good selectivity and sensitivity, and acceptable stability and reproducibility, the proposed sensor exhibited significant potential application in Pb^{2+} determination.

2. Experimental

2.1. Materials and reagents

Analytical-grade ammonium tungstate $(NH_4)_{10}H_2W_{12}O_{42}\cdot 4H_2O$ was purchased from Sinopharm Chemical Reagent Co., Ltd. (China). Ethylenediamine, lead nitrate ($Pb(NO_3)_2$) and other metal salts were purchased from Nanjing Chemical Reagent Co., Ltd. (China). Nafion (5 wt.% in lower aliphatic alcohols and water) was purchased from Sigma-Aldrich (St. Louis, MO, U.S.A.). Acetate buffer solutions (0.1 M) with different pHs were prepared by mixing the stock solutions of 0.1 M sodium acetate (CH_3COONa) and acetic acid (CH_3COOH). All other chemicals were of analytical grade and without further purification. Ultrapure water (≥18 MΩ, Milli-Q, Millipore) was used throughout the work.

2.2. Apparatus

All electrochemical experiments were performed using a CHI630D electrochemical workstation (CH Instruments Inc., U.S.A.) with a conventional three-electrode cell, in which the bare or modified glassy carbon electrode (GCE) ($d = 3$ mm), the saturated calomel electrode, and platinum wire served as the working, reference and auxiliary electrodes, respectively.

Transmission electron microscopy (TEM) images were recorded on a Model JEM 2100 high-resolution TEM microscope (JEOL, Japan). Scanning electron microscopy (SEM) images were obtained with a Hitachi Model S-4800 SEM microscope (Japan). Infrared (IR) spectra were recorded on a Nicolet NEXUS870 Fourier transform infrared (FT-IR) spectrometer (Madison, WI). X-ray photoelectron spectroscopy (XPS) experiments were conducted using a Model ESCALAB 250 spectrometer (Thermo-VG Scientific Co., U.S.A.) with an ultrahigh vacuum generator.

2.3. Preparation of WOx–EDA nanowires and modified electrode

WOx–EDA nanowires were synthesized by a facile solvothermal route according to the work reported previously [28]. In brief, $(NH_4)_{10}H_2W_{12}O_{42}\cdot 4H_2O$ (15.1 g) and ethylenediamine (60 mL) were mixed under vigorous stirring for 10 min and then transferred to a Teflon-lined stainless steel autoclave with an inner volume of 100 mL, and heated to 200 °C for 24 h, followed by natural cooling to room temperature. Here ammonium tungstate quickly transformed to an unknown intermediate at room temperature after mixing with ethylenediamine, and a large number of crystal nuclei of WOx–EDA hybrids were instantly formed. In the close system, the boiling point of ethylenediamine was higher than that at a general system, thus it could not be boiled in the Teflon-lined stainless steel autoclave [28]. The product was washed thoroughly with deionized water (until the pH reached neutral) and ethanol to remove any possible residues, and then collected by centrifugation and dried in a vacuum oven at 60 °C overnight.

The WOx–EDA-based sensor was constructed with the following procedure: first, the bare GCE was polished with 0.3 and 0.05 μm alumina slurry on microcloth pads, respectively, followed by successive sonication with pure water and ethanol for 3 min and drying with nitrogen. Meanwhile, Nafion solution was diluted to 0.5% *w*/*w* with ethanol, and varying amounts of WOx–EDA nanowires (0, 0.5, 1.0, 2.0, 4.0, or 7.0 mg) were suspended in 1 mL of 0.5% *w*/*w* Nafion solution and sonicated for 30 min to get homogeneous WOx–EDA/Nafion suspensions. Then 5 μL of this suspension was pipetted onto the GCE surface. After the solvent was evaporated, the electrode was thoroughly rinsed with deionized water and dried in a nitrogen stream.

2.4. Electrochemical detection of Pb^{2+}

Square wave anodic stripping voltammetry (SWASV) was used for the detection of Pb^{2+} under optimal conditions. The deposition step proceeded at −1.0 V for 180 s in 0.1 M acetate buffer (pH 5.0) with constant stirring. The anodic stripping of electrodeposited metal was performed in the potential range from −0.8 to −0.4 V with a frequency of 15 Hz, amplitude of 25 mV, and increment potential of 5 mV after 30 s quiescence. After each experiment the sensor was held at +0.6 V for 180 s to remove the previous deposits completely.

3. Results and discussion

3.1. Characterization of WOx–EDA nanowires

Sufficient Wox–EDA nanowires were produced by a simple and reproducible one-pot solvothermal method using commercial ammonium tungstate and ethylenediamine. SEM and TEM images were recorded to characterize the morphology and size of WOx–EDA. As shown in Fig. 1A, the as-obtained products were entirely composed of straight and uniform nanowires with length up to several micrometers. TEM image (Fig. 1B) indicated that the WOx–EDA nanowires were uniform in the diameters ranging from 50 to 150 nm, which was in good agreement with those reported previously [28]. The nanowire structure of WOx–EDA provided them a high surface-to-volume ratio, and the surface area determined by Brunauer–Emmett–Teller (BET) testing was 10.2 $m^2\ g^{-1}$.

The WOx–EDA nanowires were lamellar mesostructure with an alternate stacking of interconnected $[WO_6]$ octahedral layers and ethylenediamine monolayers. The form of the amino groups on WOx–EDA nanowires was significant to their detection performance toward Pb^{2+} because the chelating reaction could only occur between Pb^{2+} and neutral $-NH_2$ but not protonated $-NH_3^+$. The characteristic IR peak locating at 1630 cm^{-1} instead of 2100 cm^{-1} demonstrated that the amino groups on WOx–EDA nanowires were in the form of neutral $-NH_2$ rather than protonated $-NH_3^+$ (Fig. 1C). This result was further confirmed by XPS spectrum (Fig. 1D), in which the binding energy of N 1s was identical to that of alkylamine (399.6 eV), rather than that of alkylammonium (402.4 eV) [30,31]. The WOx–EDA nanowires featured with high surface-to-volume ratio and abundant neutral amino groups showed a good adsorption capacity toward Pb^{2+} in water [9,28].

3.2. Electrochemical detection of Pb^{2+} at different electrodes

To clarify the detection performance of the proposed sensor, the stripping voltammograms of 1 μM Pb^{2+} in 0.1 M NaAc–HAc (pH 5.0) at bare, Nafion, and WOx–EDA/Nafion modified GCEs were observed (Fig. 2). Compared with the response at bare GCE (curve a), the peak current increased slightly when Nafion was modified on GCE (curve b). This was probably due to the ion-exchange property of the Nafion film [27]. As a cation-exchange polymer, Nafion could provide a favorable conductive membrane matrix with anion sites for stabilizing the surface-extracted Pb^{2+} ions. Under the same condition, a well-defined peak was observed at the WOx–EDA/Nafion GCE (curve c), and the current response increased by nearly 5-fold compared to that at bare GCE,

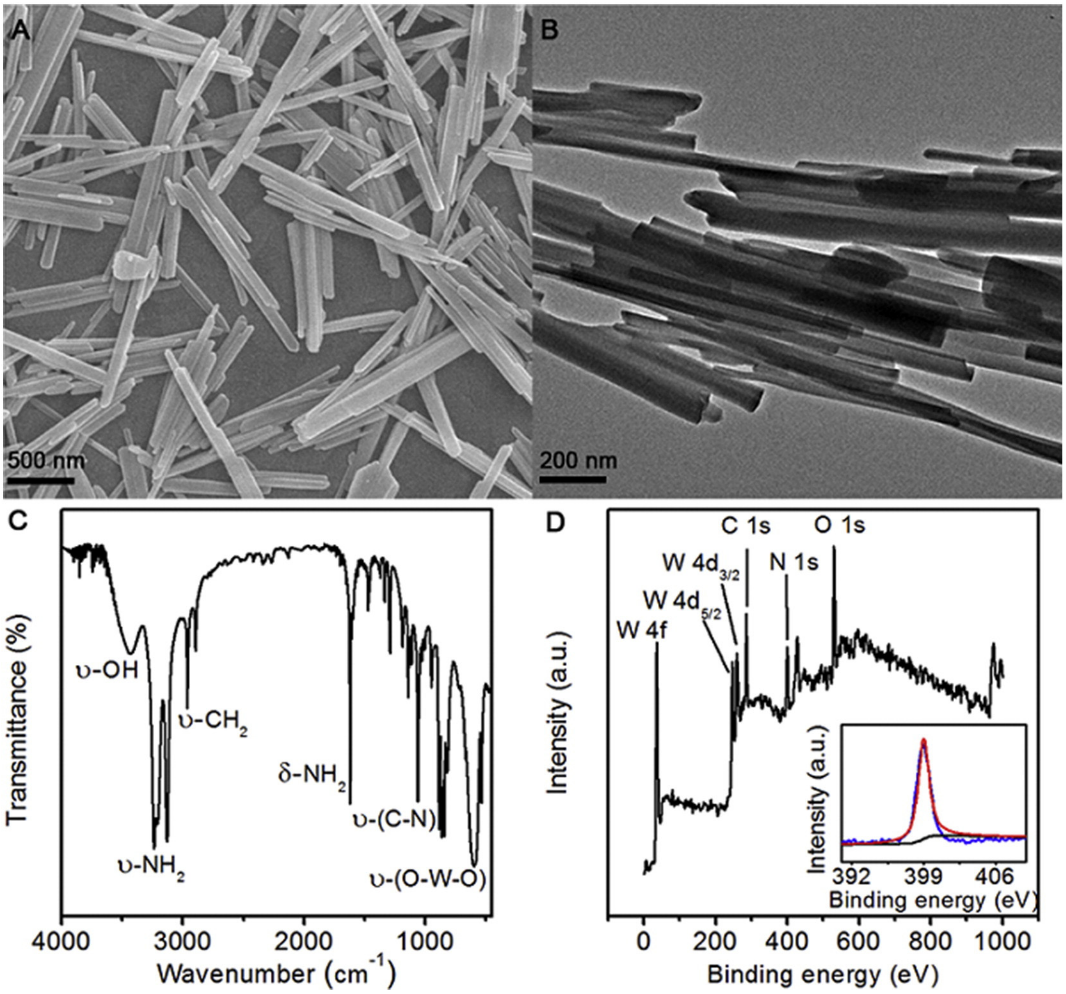

Fig. 1. (A) SEM and (B) TEM images, (C) FTIR and (D) XPS spectra of WO*x*–EDA hybrid nanowires.

indicating that the proposed sensor could be used as an enhanced electrochemical sensing platform for Pb^{2+}.

3.3. Optimization of detection conditions

In order to obtain the maximum sensitivity of trace heavy metal detection with the WO*x*–EDA/Nafion-modified GCE, some parameters such as the amount of WO*x*–EDA in 1 mL Nafion, the pH of detection solution, deposition time and deposition potential were carefully investigated under 1 μM Pb^{2+}. Since the WO*x*–EDA acted as a highly efficient adsorbent, the amount of WO*x*–EDA greatly affected the selectivity and sensitivity of the determination. With the increasing amount of WO*x*–EDA, the SWASV response of 1 μM Pb^{2+} at the modified electrode increased and reached the maximum value at 1.0 mg of WO*x*–EDA (Fig. 3A). However, the peak current conversely decreased with the further increase of the mass. This was due to the thickness increase of the WO*x*–EDA/Nafion film on the GCE surface, which consequently lowered the film conductivity. Owing to uncompensated resistive effects or lowering of the charge transfer rate, the peak currents decreased when the WO*x*–EDA/Nafion film was too thick. Therefore, 5 μL of 1.0 mg/mL WO*x*–EDA in 0.5% *w*/*w* Nafion was selected for the electrode modification.

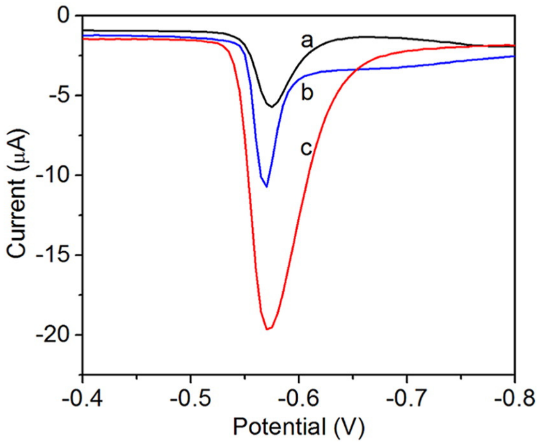

Fig. 2. SWASV analyses of (a) bare, (b) Nafion and (c) WO*x*–EDA/Nafion modified GCE in 0.1 M acetate buffer (pH 5.0) containing 1.0 μM Pb^{2+}. Deposition potential: −1.0 V, deposition time: 180 s.

The effect of solution pH on the stripping current was studied from pH 3.0 to pH 7.0 by adjusting the ratio of NaAc to HAc (Fig. 3B). At low pH values (*e.g.*, pH 3.0), the response was poor. This phenomenon could be attributed to slight protonation of the lone pair of nitrogen in the hybrid WO*x*–EDA nanowires, hindering the complexation reaction between Pb^{2+} and WO*x*–EDA at low pH. In addition, the WO*x*–EDA nanowires might also decompose to nanosheets in strongly acidic solutions (*e.g.*, pH < 3) [28]. At high pH values, the hydrolysis of Pb^{2+} interfered with the accumulation. Thus, pH 5.0 was used as the optimal pH for stripping voltammetric analysis.

The deposition time and deposition potential were very important factors for stripping voltammetric analysis. The deposition times of 60, 120, 180, 240 and 300 s were examined using SWASV in 0.1 M NaAc–

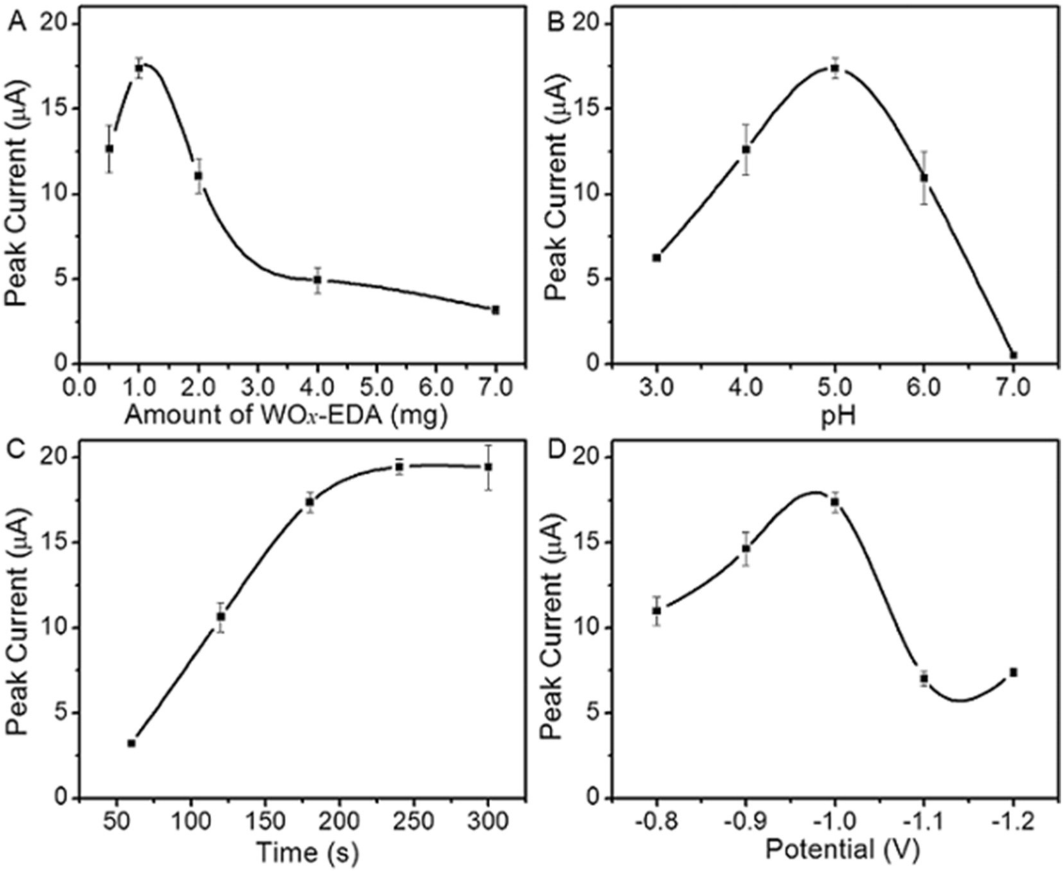

Fig. 3. Effects of (A) amount of WO*x*–EDA, (B) pH, (C) deposition time and (D) deposition potential on SWASV response of WO*x*–EDA/Nafion modified GCE in 0.1 M acetate buffer containing 1.0 μM Pb^{2+}. Results are expressed as the average of three independent experiments. Error bars represent standard deviations (SD, σ).

HAc (pH 5.0) containing 1 μM Pb^{2+} (Fig. 3C). The peak current increased sharply to 180 s, while the gradual increment trend was no longer obvious with further prolonging of the deposition time due to the surface saturation of Pb^{2+}. Thus, an optimized deposition time of 180 s was used for further studies. It should be pointed out that the deposition saturation time is inversely related to the concentration of Pb^{2+}, however, in the same order of magnitude of concentration, the difference in deposition saturation time is not significant. So, this deposition time should be also suitable for the detection of Pb^{2+} with concentrations lower than 10 μM.

In addition, the effect of exposure time before applying the deposition potential was also concerned (Fig. S1). No significant increase of the peak current was observed with a 3-min exposure before applying the deposition potential. This might be because the adsorption equilibrium could be achieved during the deposition process on behalf of the superb absorption capacity of WO*x*–EDA nanowires for Pb^{2+} in a stirring solution. So, in this work, no exposure process was taken before applying the deposition potential.

The effect of deposition potential on the peak current was also studied in the potential range from −0.8 to −1.2 V. As shown in Fig. 3D, the stripping peak current for Pb^{2+} increased and reached a maximum at −1.0 V. The response decreased at deposition potentials more negative than −1.0 V as a result of the competitive reduction of hydrogen ions and hydrogen bubbling on the surface of the electrode at these potentials, which made the electrode surface passive. Therefore, −1.0 V was chosen as the optimal deposition potential throughout.

3.4. Analytical performance

The SWASV responses of the WO*x*–EDA-based sensor toward Pb^{2+} were recorded as shown in Fig. 4. The stripping peak current of Pb^{2+} was positively proportional to its concentration from 0.01 to 10 μM (2.07 μg L^{-1} to 2.07 mg L^{-1}) (Fig. 4A). The plot of peak current *versus* concentration exhibited good linearity with a sensitivity of 14.35 μA μM^{-1} and a correlation coefficient of 0.9937 (Fig. 4B). The limit of detection at 3σ was calculated to be 3.2 nM (0.66 μg L^{-1}), which was much lower than the guideline value for drinking water given by the World Health Organization (WHO) (10 μg L^{-1}) [32]. The analytical performance was also compared with other modified electrodes reported previously, which were summarized in Table 1.

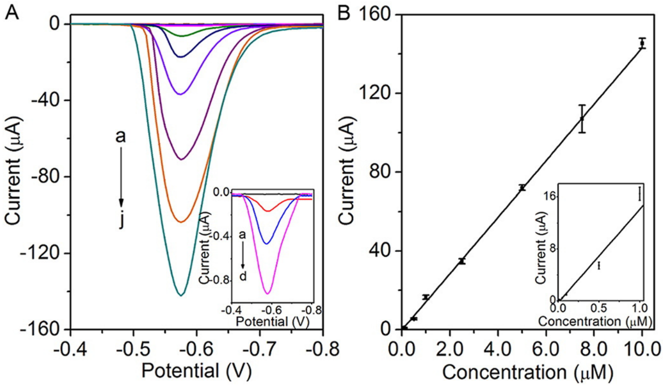

Fig. 4. (A) SWASV responses of the WO*x*–EDA/Nafion modified GCE to Pb^{2+} at 0, 0.01, 0.05, 0.1, 0.5, 1.0, 2.5, 5.0, 7.5, and 10.0 μM (from a to j). (B) The corresponding calibration curve. Inset: SWASV and calibration curves at 0.01–0.1 μM Pb^{2+}. Results are expressed as the average of three independent experiments. Error bars represent standard deviations (SD, σ).

3.5. Selectivity, stability and reproducibility

The selectivity of the proposed sensor was investigated by measuring the SWASV stripping responses toward Pb^{2+} along with some common heavy metal ions such as Zn^{2+}, Cd^{2+}, Cu^{2+}, and Hg^{2+}. Fig. 5 shows the SWASV signals of bare and WOx–EDA/Nafion GCEs toward 0.1 M acetate buffer (pH 5.0) containing the five heavy metal ions at 1.0 μM. At bare GCE all these ions showed their stripping peaks, and the small peak beside the peak to Pb^{2+} might be attributed to the stripping of Pb from the Pb-amalgam formed during deposition, while the WOx–EDA/Nafion GCE showed only a large and well-defined stripping peak toward Pb^{2+}, which was much higher than that toward other four ions. The selective detection of Pb^{2+} could be attributed to the excellent adsorption of Pb^{2+} over other ions by the WOx–EDA nanowires.

The interference study was also conducted by measuring the SWASV stripping responses of the WOx–EDA/Nafion GCE toward Pb^{2+} in the presence of several possible interfering metal ions (*e.g.*, Mg^{2+}, Al^{3+}, Fe^{3+}, Zn^{2+}, Co^{2+}, Ni^{2+}, Cu^{2+}, Hg^{2+}, Cd^{2+}, Mn^{2+}) at the ten times higher concentration comparatively. As shown in Fig. 6, except Cu^{2+} and Hg^{2+} no significant influence on stripping peak current was observed with deviation below 5%, even though over 10-fold other ions were added into the solution, which was because of the highly selective adsorption of Pb^{2+} on the WOx–EDA nanowires, thus causing an excellent selectivity for stripping sensing Pb^{2+}. Mercury ions could be reduced and formed a film on the surface of electrode, which caused Pb^{2+} to be reduced more easily by forming an amalgam [44]. As a result, a considerable increase of the stripping peak current was found when high concentration of Hg^{2+} was added. The ion influence can be eliminated by applying the standard addition method [9,22,41]. Meanwhile, the SWASV signal for Pb^{2+} was diminished by 35% in the presence of Cu^{2+}, because of the formation of a Pb–Cu intermetallic compound [45]. The interference of Cu^{2+} could be excluded by Ferricyanide [46]. The interferences from surfactants such as Triton X-100, Tween-20 (non-ionic surfactants), sodium dodecyl sulfate (SDS, anionic surfactant) and cetyltrimethyl ammonium bromide (CTAB, cationic surfactant) were also studied. No significant change of the peak current of Pb^{2+} was observed even in the presence of surfactant at ten times higher concentrations than Pb^{2+} (Fig. S2).

In the view of practical analytical application, the repeatability of the proposed sensor was evaluated by repetitively detecting 1.0 μM Pb^{2+}, giving the relative standard deviation (RSD) of 6.5% ($n = 10$). In addition, the sensor was proved to have long-term stability for dealing with the deposition and stripping procedure. The response maintained a value of more than 95% over 30 days. The reproducibility of the sensor fabrication was also investigated. Six identical sensors were prepared in the same condition and then evaluated by performing determination of Pb^{2+}. The RSD value turned out to be 5.3%. Additionally, the electrode could be easily regenerated by applying a positive potential of +0.6 V. The high stability and reproducibility made the proposed sensor potentially useful for the analysis of real samples.

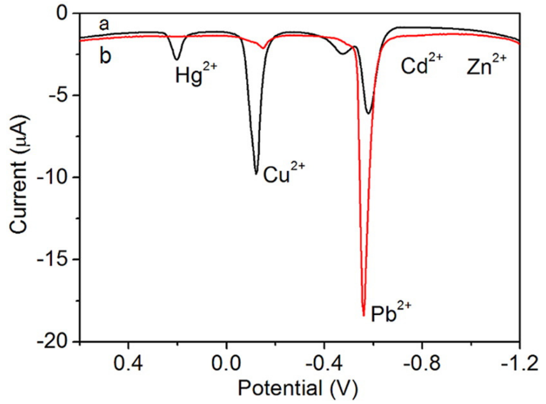

Fig. 5. SWASV stripping responses at (a) bare and (b) WOx–EDA/Nafion modified GCE toward 0.1 M acetate buffer (pH 5.0) containing five heavy metal ions (Pb^{2+}, Zn^{2+}, Cd^{2+}, Cu^{2+}, Hg^{2+}) at 1.0 μM. Stripping potential range: −1.2 to +0.6 V, other conditions are identical to those in Fig. 2.

3.6. Real sample analysis

In order to evaluate the practicability of the proposed method, the analyses of real water samples have been carried out without any pretreatment except filtration through a 0.2 μm membrane. The samples were collected from laboratory tap water and Qinhuai River in Nanjing, China. It turned out that no obvious signal for Pb^{2+} was observed, suggesting that the concentration of Pb^{2+} in the samples was extremely low. For this reason, different concentrations of Pb^{2+} were spiked into these samples for recovery evaluation [8,9]. The SWASV responses and detection results along with the recoveries were shown in Fig. S3 and Table 2, respectively. The average recoveries were in the range from 95.4% to 107.1% for three determinations, demonstrating satisfactory accuracy of the proposed method for the determination of Pb^{2+} in real samples.

Table 1
Comparison of Pb^{2+} sensing performance of this work with the previous works using other materials.

Electrode	Modifier	Detection range (μM)	LOD[a] (μM)	Ref.
GCDE[b]	Mercury film	0.048–0.48	0.01	[33]
GCE	Antimony film	0.1–0.7	0.0043	[34]
SPCE[c]	Bismuth film	0–0.62	0.0062	[35]
GCE	Nafion–Bi film	0.01–0.3	0.01	[36]
GCE	MWCNTs[d]	0.02–10	0.004	[37]
CPE[e]	MWCNTs/nanosilica	$0.1–10^4$	0.073	[38]
CPE	MWCNTs/Amberlite IR-120	0.096–1.7	0.021	[39]
SPCE	Heated graphite nanoparticle	0.024–0.48	0.015	[40]
CPE	MOF-5[f]	0.01–1	0.0049	[41]
CPE	Zeolite NH_4-Y	0.025–0.1	0.017	[42]
GCE	TCA[g]	0.1–25	0.008	[43]
GCE	WOx–EDA/Nafion	0.01–10	0.0032	This work

[a] Limit of detection.
[b] Glassy carbon disk working electrode.
[c] Screen-printed carbon electrode.
[d] Multiwalled carbon nanotubes.
[e] Carbon paste electrode.
[f] Metal-organic framework.
[g] *p-tert*-Butylthiacalix[4]arene.

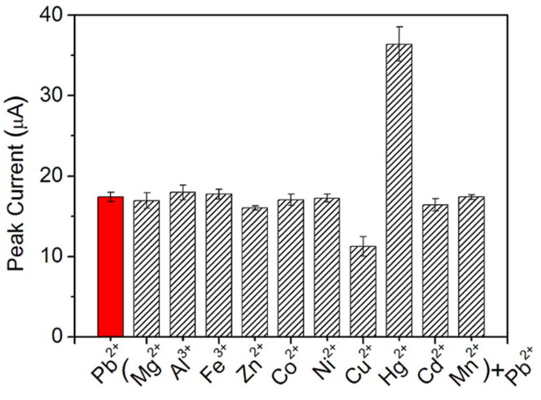

Fig. 6. Interference study of the WOx–EDA/Nafion modified GCE in 0.1 M acetate buffer (pH 5.0) containing 1.0 μM Pb^{2+} without and with 10.0 μM Mg^{2+}, Al^{3+}, Fe^{3+}, Zn^{2+}, Co^{2+}, Ni^{2+}, Cu^{2+}, Hg^{2+}, Cd^{2+} or Mn^{2+}. SWASV conditions are identical to those in Fig. 2.

Table 2
Determination of Pb^{2+} in water samples using the WO*x*–EDA/Nafion modified electrode.

Samples	Add (nM)	Result (nM)	Recovery (%)
Tap water 1	50.0	50.3 ± 2.8	100.6
Tap water 2	100.0	95.8 ± 5.4	95.8
River water 3	50.0	53.5 ± 2.8	107.1
River water 4	200.0	190.8 ± 7.0	95.4

4. Conclusion

A highly selective and sensitive electrochemical sensor for Pb^{2+} was proposed by using WO*x*–EDA hybrid nanowires as electrode modification material. The WO*x*–EDA nanowires showed a uniform lamellar mesostructure and were rich with neutral amino groups. Due to the high surface-to-volume ratio and the chelating effect between amino groups and Pb^{2+}, WO*x*–EDA nanowires exhibited superb absorption capacity toward Pb^{2+}. The WO*x*–EDA-based sensor showed good analytical performance of wide linear range, low detection limit, nice selectivity and good reproducibility and accuracy for Pb^{2+}. This work provided a promising analytical approach for Pb^{2+} determination in water samples and broadened the application of inorganic–organic hybrid materials in electrochemical sensing of heavy metal ions in environmental samples.

Acknowledgments

We gratefully acknowledge the National Special Project for Key Scientific Apparatus Development (2012YQ170000302), National Natural Science Foundation of China (21135002 and 21361162002), and Priority development areas of The National Research Foundation for the Doctoral Program of Higher Education of China (20130091130005).

Appendix A. Supplementary data

Supplementary data to this article can be found online at http://dx.doi.org/10.1016/j.jelechem.2015.09.001.

References

[1] M. Tuzen, E. Melek, M. Soylak, J. Hazard. Mater. 136 (2006) 597–603.
[2] M. Kobya, E. Demirbas, E. Senturk, M. Ince, Bioresour. Technol. 96 (2005) 1518–1521.
[3] H.L. Needleman, P.J. Landrigan, Am. J. Public Health 94 (2004) 8.
[4] D.I. Bannon, C. Murashchik, C.R. Zapf, M.R. Farfel, J.J. Chisolm, Clin. Chem. 40 (1994) 1730–1734.
[5] P. Ugo, S. Zampieri, L.M. Moretto, D. Paolucci, Anal. Chim. Acta 434 (2001) 291–300.
[6] K.W. Huang, C.J. Yu, W.L. Tseng, Biosens. Bioelectron. 25 (2010) 984–989.
[7] L.X. Xie, Y. Qin, H.Y. Chen, Anal. Chem. 84 (2012) 1969–1974.
[8] L. Cui, J. Wu, H.X. Ju, ACS Appl. Mater. Interfaces 6 (2014) 16210–16216.
[9] R.X. Xu, X.Y. Yu, C. Gao, J.H. Liu, R.G. Compton, X.J. Huang, Analyst 138 (2013) 1812–1818.
[10] L. Cui, J. Wu, H.X. Ju, Biosens. Bioelectron. 63 (2015) 276–286.
[11] D. Dragoea, N. Spătarub, R. Kawasakia, A. Manivannanc, T. Spătarub, D.A. Trykd, A. Fujishimae, Electrochim. Acta 51 (2006) 2437–2441.
[12] M. Javanbakht, F. Divsar, A. Badiei, F. Fatollahi, Y. Khaniani, M.R. Ganjali, P. Norouzi, M. Chaloosi, G.M. Ziarani, Electrochim. Acta 54 (2009) 5381–5386.
[13] Z.Q. Zhao, X. Chen, Q. Yang, J.H. Liu, X.J. Huang, Chem. Commun. 48 (2012) 2180–2182.
[14] L. Zhu, L.L. Xu, B.Z. Huang, N.M. Jia, L. Tan, S.Z. Yao, Electrochim. Acta 115 (2014) 471–477.
[15] L.L. Xiao, H.B. Xu, S.H. Zhou, T. Song, H.H. Wang, S.Z. Li, W. Gan, Q.H. Yuan, Electrochim. Acta 143 (2014) 143–151.
[16] H. Lina, M.X. Li, D. Mihailovic, Electrochim. Acta 154 (2015) 184–189.
[17] F. Ke, L.G. Qiu, Y.P. Yuan, F.M. Peng, X. Jiang, A.J. Xie, Y.H. Shen, J.F. Zhu, J. Hazard. Mater. 196 (2011) 36–43.
[18] S.H. Huang, D.H. Chen, J. Hazard. Mater. 163 (2009) 174–179.
[19] A. Bagheri, M. Taghizadeh, M. Behbahani, A.A. Asgharinezhad, M. Salarian, A. Dehghani, H. Ebrahimzadeh, M.M. Amini, Talanta 99 (2012) 132–139.
[20] N. Yee, L.G. Benning, V.R. Phoenix, F.G. Ferris, Environ. Sci. Technol. 38 (2003) 775–782.
[21] F. Ge, M.M. Li, H. Ye, B.X. Zhao, J. Hazard. Mater. 211 (2012) 366–372.
[22] D.W. Pan, Y.E. Wang, Z.P. Chen, T.T. Lou, W. Qin, Anal. Chem. 81 (2009) 5088–5094.
[23] K.H. Park, J.W. Choi, J.S. Chun, H.J. Kim, S.U. Son, Chem. Commun. 1660 (2008) 1659–1661.
[24] N.S. Gadhari, B.J. Sanghavi, S.P. Karna, A.K. Srivastava, Electrochim. Acta 56 (2010) 627–635.
[25] W.F. Deng, Y.M. Tan, Y.Y. Li, Y.Q. Wen, Z.H. Su, Z. Huang, S.Q. Huang, Y. Meng, Q.J. Xie, Y.P. Luo, S.Z. Yao, Microchim. Acta 169 (2010) 367–373.
[26] X.L. Shao, H. Gu, Z. Wang, X.L. Chai, Y. Tian, G.Y. Shi, Anal. Chem. 85 (2013) 418–425.
[27] Y. Wei, R. Yang, X.Y. Yu, L. Wang, J.H. Liu, X.J. Huang, Analyst 137 (2012) 2183–2191.
[28] W. Li, F. Xia, J. Qu, P. Li, D.H. Chen, Z. Chen, Y. Yu, Y. Lu, R.A. Caruso, W.G. Song, Nano Res. 7 (2014) 903–916.
[29] C. Gao, X.Y. Yu, S.Q. Xiong, J.H. Liu, X.J. Huang, Anal. Chem. 85 (2013) 2673–2680.
[30] L. Yu, R.J. Zou, Z.Y. Zhang, G.S. Song, Z.G. Chen, J.M. Yang, J.Q. Hu, Chem. Commun. 47 (2011) 10719–10721.
[31] Q.S. Gao, P. Chen, Y.H. Zhang, Y. Tang, Adv. Mater. 20 (2008) 1837–1842.
[32] P. Chooto, P. Wararatananurak, C. Innuphat, ScienceAsia 36 (2010) 150–156.
[33] S. Suteerapataranon, J. Jakmunee, Y. Vaneesorn, K. Grudpan, Talanta 58 (2002) 1235–1242.
[34] S.B. Hocevar, I. Svancara, B. Ogorevc, K. Vytras, Anal. Chem. 79 (2007) 8639–8643.
[35] S. Chuanuwatanakul, W. Dungchai, O. Chailapakul, S. Motomizu, Anal. Sci. 24 (2008) 589–594.
[36] G. Kefala, A. Economou, Anal. Chim. Acta 576 (2006) 283–289.
[37] K.B. Wu, S.S. Hu, J.J. Fei, W. Bai, Anal. Chim. Acta 489 (2003) 215–221.
[38] M.R. Ganjalia, N. Motakef-Kazamia, F. Faridbod, S. Khoee, P. Norouzi, J. Hazard. Mater. 173 (2010) 415–419.
[39] M.E. Nascimento, P.B. Martelli, C.A. Furtado, A.P. Santos, L.F. Oliveira, H.F. Gorgulho, Microchim. Acta 173 (2011) 485–493.
[40] G. Aragay, J. Pons, A. Merkoc, J. Mater. Chem. 21 (2011) 4326–4331.
[41] Y. Wang, Y.C. Wu, J. Xie, X.Y. Hu, Sensors Actuators B 177 (2013) 1161–1166.
[42] S. Senthilkumar, R. Saraswathi, Sensors Actuators B 141 (2009) 65–75.
[43] H. Zheng, Z.N. Yan, H.M. Dong, B.X. Ye, Sensors Actuators B 120 (2007) 603–609.
[44] J. Schiewe, K.B. Oldham, J.C. Myland, A.M. Bond, V.A. Vicente-Beckett, S. Fletcher, Anal. Chem. 69 (1997) 2673–2681.
[45] R.J. Grim, J. Phys. Chem. 46 (1942) 464–469.
[46] R.O. Kadara, I.E. Tothill, Talanta 66 (2005) 1089–1093.